frontiers | Frontiers in Mechanical Engineering

TYPE Review
PUBLISHED 08 September 2022
DOI 10.3389/fmech.2022.981846

OPEN ACCESS

EDITED BY
Amit Bandyopadhyay,
Washington State University,
United States

REVIEWED BY
Manikandan M,
Vellore Institute of Technology, India

*CORRESPONDENCE
Sajan Kapil,
sajan.kapil@iitg.ac.in

SPECIALTY SECTION
This article was submitted to Digital Manufacturing,
a section of the journal
Frontiers in Mechanical Engineering

RECEIVED 29 June 2022
ACCEPTED 10 August 2022
PUBLISHED 08 September 2022

CITATION
Kapil S, Rajput AS and Sarma R (2022), Hybridization in wire arc additive manufacturing.
Front. Mech. Eng 8:981846.
doi: 10.3389/fmech.2022.981846

Hybridization in wire arc additive manufacturing

Sajan Kapil*, Atul Singh Rajput and Ritam Sarma

Indian Institute of Technology Guwahati, Guwahati, India

Wire Arc Additive Manufacturing (WAAM) can produce a near-net shape of an object within a short period due to its capability of high deposition rate compared with other metal Additive Manufacturing (AM) processes. The recent developments in the WAAM have increased its efficiency and cost-effectiveness in producing viable products. However, poor surface quality, porosities, residual stresses, distortions, and anisotropic mechanical properties are a few inherent challenges still associated with the WAAM, which necessitates the hybridization of this process. Hybrid-WAAM is a synergic integration of one or more deposition processes, manufacturing processes, layering strategies, raw stock materials, and machine tool kinematics that are fully coupled and affect part quality, functionality, and process performance. This paper comprehensively reviews different levels of hybridization in the WAAM to eliminate its associated challenges. These levels of hybridizations are classified into five categories: hybrid-deposition processes, hybrid-manufacturing processes, hybrid-layering strategies, hybrid-machine tools, and hybrid-raw stock. Furthermore, these levels of hybridization are mapped to eliminate the associated defects/challenges in the WAAM, which will help the readers select an appropriate level of hybridization.

KEYWORDS

wire arc additive manufacturing, hybrid-deposition processes, hybrid-manufacturing processes, hybrid-layering strategies, hybrid-machine tools, hybrid-raw stock

1 Introduction

Wire Arc Additive Manufacturing (WAAM) is a disruptive process for fabricating metal 3D objects layer-by-layer. The history of WAAM can be traced from a patent filed in 1925 claiming the use the welding for fabricating decorative 3D objects (Baker, 1925). However, the progressive development of WAAM for metal object fabrication started in the 90s when several research groups started focusing on this topic. Since then, several innovations have been associated with WAAM for metal parts fabrications (Derekar, 2018). Among seven AM processes by ASTM 2009 (Zhang et al., 2002), WAAM is one kind of DED process known for its capability of fabricating large metallic objects with lower built time. In any WAAM setup, three primary units are used: 1) Deposition Unit, 2) Motion Kinematics Unit, and 3) Control Unit. A deposition unit retrofitted with the motion kinematic unit deposit the molten metal in the desired area of the substrate. A control unit manipulates all the synergic motion between deposition unit substrate. In previous studies, several arc welding processes such as Metal Inert Gas (MIG), Tungsten

Inert Gas (TIG), Plasma Arc Welding (PAW), etc., (shown in Figure 1), have been explored and retrofitted with different kinds of motion kinematics units such as CNC or Robotic Arms, etc. A classification for WAAM can be drawn based on the primary unit being used, as demonstrated in Figure 2. In recent years, the development of the MIG-WAAM setup with a high degree of freedom provides ease of control during the layer-by-layer manufacturing process (Kapil et al., 2018b; Warsi et al., 2022; Kozamernik et al., 2020; Artaza et al., 2020a; Kapil et al., 2018a). Xiong et al. (2017a) conducted experiments to investigate the impact of inclination angle on the wire feed rate, travel speed, and offset distance during MIG-WAAM and observed that the inclinational angle is directly proportional to travel speed and wire feed rate, respectively. Cold Metal Transfer (CMT), reciprocation of the consumable wire feed, is used to have control and efficient heat transfer during the deposition. Shukla et al. (2020) observed that the plasma distribution width is directly proportional to the welding current during the CMT responsible for the widening of the arc. Similarly, TIG-WAAM offers precise control over the bead and stable arc compared with other WAAM setups (Geng et al., 2017; Zhang et al., 2019a; Xiong et al., 2019; Negi et al., 2020; Veiga et al., 2020). Dinovitzer et al. (2019) performed experiments to analyze the impact of the process parameters during the TIG-WAAM and observed that the surface roughness and the melting depth during the deposition primarily depend on the current applied and are independent of the wire feed rate. However, the Omni directionality issues restrict its application in robotic cells. Therefore, limited literature has been found on TIG-WAAM setups (Bai et al., 2018) (Suárez et al., 2021). For the same reason, works utilizing PAW-based WAAM setup are also minimal (Zhang et al., 2021a) (Artaza et al., 2019). The scope of any WAAM process depends on its primary units, and the classification of WAAM based on the heat source is illustrated in Figure 3. For example, compared to TIG and PAW, MIG is considered for high deposition but low surface finish. In addition to this, CNC kinematics is known for the limited size of an object compared to robotics motion kinematics. The automated WAAM process involves a sequence of steps for obtaining the required build characteristics. Initially, the CAD model for the final build is made, followed by its layer-by-layer slicing; each layer is deposited with the assistance of a selective deposition unit, adjusting the orientation and position of the substrate till the final part is fabricated. WAAM is characterized by high deposition rates, capacity to manufacture larger geometries, compatibility with different arc heat sources, as well as weld torch movements and alignments.

Poor surface quality, porosities, residual stresses, distortions, and anisotropic mechanical properties are a few inherent challenges still associated with the WAAM, which necessitates the hybridization of this process. In the WAAM process, precise material deposition is difficult due to its quality of high deposition rate. Furthermore, residual stresses are a significant issue associated with the WAAM process due to the thermal cycle of heating and cooling before and after deposition, respectively. Moreover, the porosities are generated due to raw material or the process itself. Any kind of contamination such as moisture, grease, or any other hydrocarbon associated with raw material wire or substrate may lead to porosity. However, the parts produced by WAAM have anisotropic material properties. For example, the strength of the WAAM parts is typically lower in the build direction than in the other directions. Hybrid Wire Arc Additive Manufacturing (hybrid-WAAM) is synergic and fully coupled conventional WAAM with other processes to enhance part functionality, quality, and performance. These key hybridization features are illustrated in Figure 4A. Fully coupling the processes with WAAM is labeled as the first key feature of hybrid-WAAM. Post and pre-processes of WAAM are not considered coupled, e.g., heat-treatment of the parts fabricated by WAAM to enhance the mechanical properties is a post-processing technique and will not be considered a hybrid process. The next feature of the hybrid-WAAM defines the *synergistic* nature between the two or more processes. The synergic action must lead to an increase in the output unattainable by an individual process. For example, WAAM can produce parts with less material wastage but bad surface quality; conversely, a CNC machining process can fabricate parts with excellent surface quality but high material wastage. A hybridization between CNC machining and WAAM can eliminate the limitations and unify the advantages associated

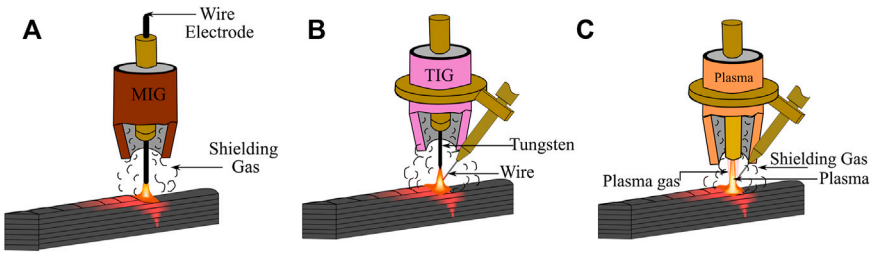

FIGURE 1
Working principle of **(A)** Metal Inert Gas (MIG) Welding, **(B)** Tungsten Inert Gas (TIG) Welding, and **(C)** Plasma Arc Welding (PAW).

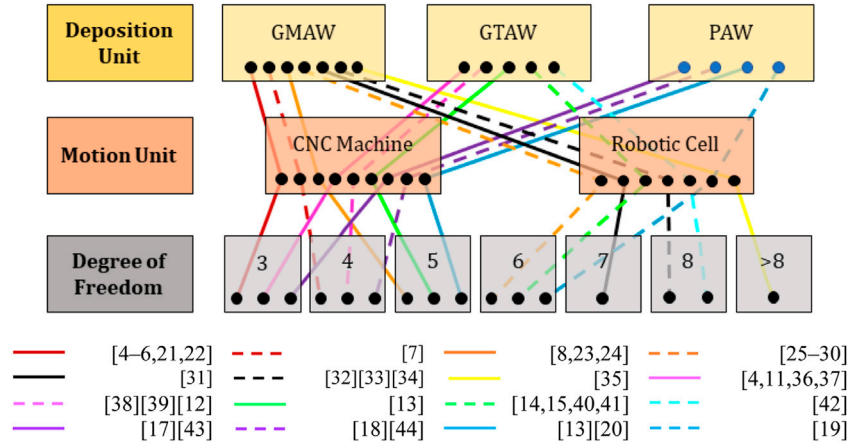

FIGURE 2
Classification of WAAM setups.

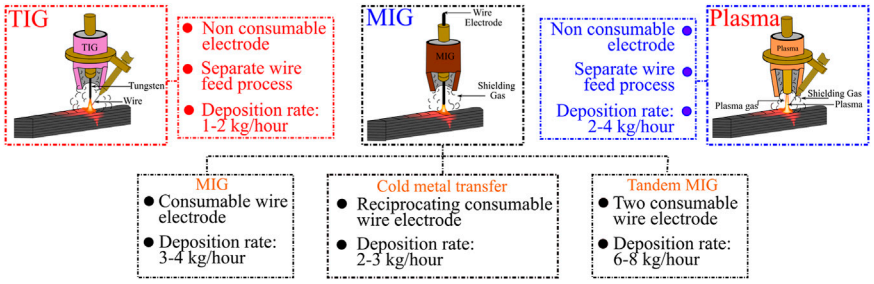

FIGURE 3
Classification based on different heat sources utilized in WAAM.

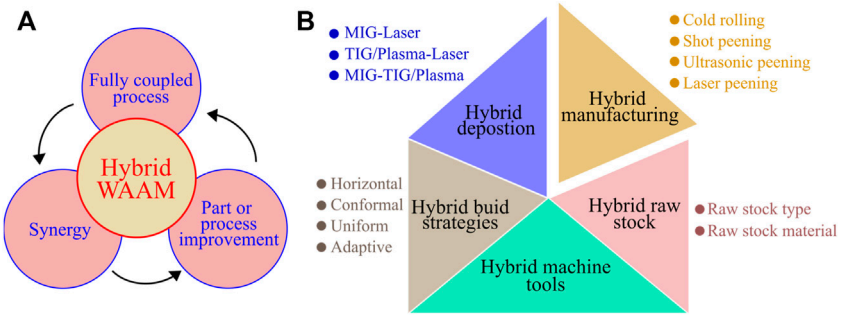

FIGURE 4
(A) Features and **(B)** levels of hybrid-WAAM.

with each other. The last feature of this definition relates to the effect of the hybridization on the part functionality, process quality, and performance. For example, hybridizing WAAM and laser shock pinning will enhance the fatigue life of the produced parts. The improved quality of the fabricated parts leads to a decreased time to market (Williams et al., 2016). Furthermore, Hybrid-WAAM is a promising alternative for fabricating components made of expensive materials such as titanium and nickel in the aerospace industry, where such components often suffer a highly high buy-to-fly ratio (Ding et al., 2015a). Moreover, the large-scale metallic structures can be easily fabricated through the Hybrid-WAAM, enhancing manufacturing efficiency and reducing material waste (Marinelli et al., 2019).

Over the period, several research groups have utilized the benefits of hybridization in WAAM. However, little literature is available discussing the evolution and levels of hybridization in WAAM. Therefore, this paper uniquely categorizes the levels of hybridization into five groups: hybrid-deposition processes, hybrid-manufacturing processes, hybrid-layering strategies, hybrid-machine tools, and hybrid-raw stock. These levels of hybrid-WAAM are shown in Figure 4B. These levels of hybridization can eliminate the associated defects/challenges in the WAAM, which will help select an appropriate level of hybridization. Therefore, the primary defects/challenges associated with WAAM are discussed in the next Section 2, and different levels of hybridization are addressed in Section 3. Finally, in Section 4, a discussion has been provided to select an appropriate level of hybridization to eliminate the challenges of WAAM.

2 Challenges in wire arc additive manufacturing

2.1 Productivity

Owing to the higher deposition rate, WAAM is taking over the metal AM industry for the realization of medium to larger-scaled metallic components. The associated welding process primarily governs the deposition rate. MIG-WAAM has been observed to yield a deposition rate varying from 1 kg/h to 4 kg/h (Williams et al., 2016) (Paskual et al., 2018). However, this leads to poor geometrical accuracy of the deposited part. The issue can be eliminated by adopting TIG-WAAM with a deposition rate of 1.5–2 kg/h. The selection of optimized process parameters yields bridge transfer resulting smooth bead profile in the case of TIG-WAAM. Moreover, spatters in the deposited bead were also reduced because of the improved stability of the arc. PAW-based WAAM reports a deposition rate of 3.5–4 kg/h (Artaza et al., 2020b), which can be further improved using higher diameter feedstock (Wang et al., 2021a). Many researchers have attempted to enhance the deposition rate of WAAM further. Using two electrodes in one molten pool has resulted in a higher deposition rate. However, the interfacial arc between the two electrodes leads to the induction of magnetic force (Kim et al., 2021). This induced magnetic force affected the stability of the molten pool causing poor bead morphology and increased spatters. The issue can be overcome by adding additional filler wire between trailing and leading electrodes with reverse polarity (Arita et al., 2009). So it can be noted that the higher deposition, with better geometrical accuracy, is one of the biggest challenges to achieve in WAAM.

2.2 Surface roughness

In the WAAM process, precise material deposition is difficult due to its quality of high deposition rate. Similar to other AM processes, poor surface roughness is a major challenge for the WAAM. The surface irregularities produced due to the staircase effect predominate as the thicker layer deposition of about 1–3 mm (Zhang et al., 2002; Nilsiam et al., 2017; Derekar, 2018; Wu et al., 2020; Jafari et al., 2021) is attained during WAAM. Heat input during the deposition of the material affects the bead geometry, so achieving the required dimension becomes difficult. Wu et al. (2017) have shown in their study that heat accumulation during multilayer deposition width of the deposited wall varies along the deposition direction. Dimensional accuracy in WAAM is also affected by distortion of the part due to poor heat management, as shown in Figure 5A. In addition, deposited height is different at start and end conditions as more heat sink is available at the start, and molten material tends to flow at the end, as illustrated in Figure 5B. So it can be noted that the WAAM systems, capable of producing parts with better surface finish, are required.

2.3 Residual stresses and distortion

Residual stresses are a significant issue associated with the WAAM process due to the thermal cycle of heating and cooling before and after deposition, respectively. Subsequently, distortion after unclamping the part due to the release of these residual stress occurs, as shown in Figure 5E. Typically, this distortion is quantified from the out-of-plane distance from the deposited layer (Colegrove et al., 2013; Busachi et al., 2015; Wu et al., 2015; Ning and Cong, 2016; Zhou et al., 2017). Several studies have concluded that residual stress in deposited layers and baseplate are tensile and compressive, respectively (Colegrove et al., 2013; Szost et al., 2016; Srivastava et al., 2020). The amount of residual stress depends on the type of material being deposited and can be 60% or sometimes 100% to yield the strength of the materials (Srivastava et al., 2020). Szost et al. (2016) reported tensile residual stress of about 480 MPa and out-of-plane distortion

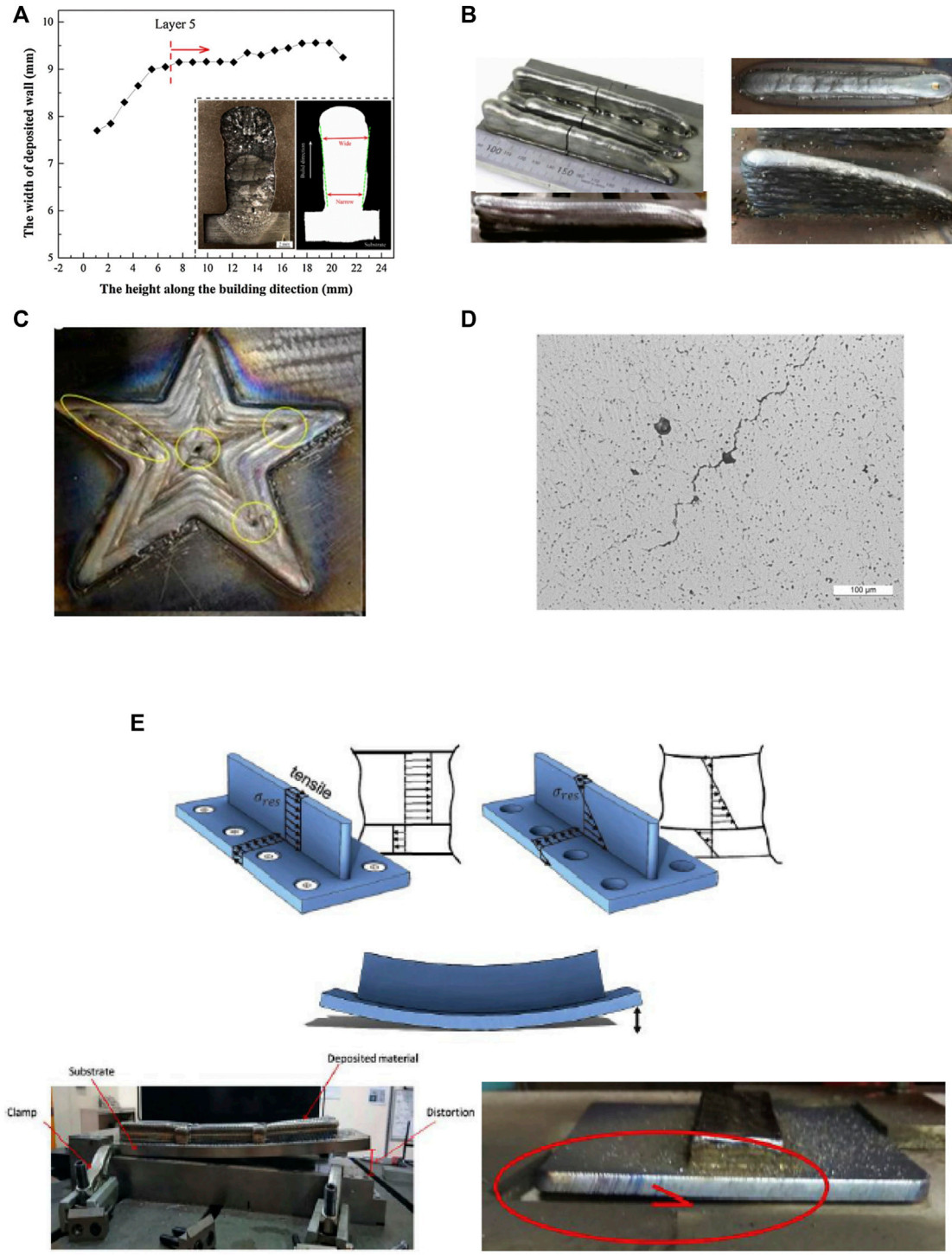

FIGURE 5
Challenges in the WAAM process: **(A)** Variation in the width of a wall deposited by TIG (Wu, 2017), **(B)** variation in height at start and end due to difference in heat dissipation, **(C)** porosities due to poor path planning (Liu et al., 2020), **(D)** porosity and crack (Gu et al., 2016) **(E)** distortion (Jafari (2021).

in the range of 7 mm for Ti6Al4V material built from a TIG-WAAM system. Similarly, Colegrove et al. (2013) reported residual stress of about 600 MPa for Steel parts made from MIG. Such a high amount of residual stress can result in distortion, crack, or delamination initiations between the layers, which affect the final mechanical properties of the build parts, as shown in Figure 5E (Xiong et al., 2017b; Nilsiam et al., 2017; Wu et al., 2020; Jafari et al., 2021). So it is desirable to produce residual stress-free objects by WAAM.

2.4 Mechanical and microstructure properties

The various defects, including anisotropy, porosity, cracks, delamination, etc., produced during the fabrication of parts through WAAM is a major limitation. The parts produced by WAAM have anisotropic material properties. For example, the strength of the WAAM parts is typically lower in the build direction than in the other directions. However, the hardness increases as grain size decrease along the build direction. The hardness is lower in the bottom region of the deposited material (nearer to the substrate) compared with the top layer (a few last deposited layers). It is because the newly deposited layer reheat the previous layers, and hence the bottom layers undergo multiple thermal cycles (heating and cooling). Therefore, due to the involvement of multiple thermal cycles, the grains of the bottom layers increase in size. A similar phenomenon was reported by Surya et al. (Suryakumar et al., 2013) in the case of the wire arc additive manufacturing of mild steel. However, the grain structures highly depend upon the thermal cycle's complexity and material properties; hence, this variation may not follow the same trend (Ahsan et al., 2020). Hence, it can be concluded that most of the products fabricated by WAAM are subjected to a variation in hardness in the build direction.

The porosities are generated due to raw material or the process itself. Any kind of contamination such as moisture, grease, or any other hydrocarbon associated with raw material wire or substrate may lead to porosity, as illustrated in Figures 5C,D (Busachi et al., 2015; Fang et al., 2018; Li et al., 2019; Derekar et al., 2020; Fu et al., 2021; Hauser et al., 2021). In addition, inappropriate process parameters can result in the poor formation of the molten pool and eventually results in porosity in build parts. Another source of porosity can be due to poor path planning. Among several materials such as Ti6Al4V, steel, Inconel, etc. Aluminum is more susceptible to gas porosities due to hydrogen contamination (Guo et al., 2022). In a study by Cong et al., round shape gas porosities of 10–50 μm size were observed in the Aluminum part build of the TIG-WAAM process (Cong et al., 2014). Porosity leads to a decrease in the mechanical strength and fatigue properties through the propagation of microcracks. Porosity may induce from either the raw materials or the deposition process. Porosity induced from the raw material result from the surface contamination of the raw materials (Wire and substrate), such as moisture, oils, and lubricating fluids, which are difficult to remove completely. These impurities get trapped in the 12 molten metal pools resulting in porosity after solidification. Process-induced porosities have resulted from poor path planning and an unstable deposition process. Inadequate fusion or spatter injection is formed in case of a complex deposition path which leads to a void or gap in that influenced region.

Similarly, cracks and delamination occur in the WAAM fabricated parts due to the deposited metals' thermal stress and material characteristics (Yuan et al., 2016a; Dong et al., 2017; Gu et al., 2018). Cracks may be classified into solidification and grain boundary cracks (Sames et al., 2016). Solidification cracks occur because of the solidified grain flow obstacle or the melt pool's high strain. On the other hand, grain boundary cracks occur due to the difference between the grain boundary morphology and potential precipitate formation along the grain boundaries (Davis, 2004). At the same time, the delamination of the layers results from the inadequate melting of the underlying layers. Furthermore, removing porosity, cracks, and anisotropy from the deposited material enhances the functionality of the WAAM object.

2.5 Multi-material objects

Multi-material objects are appropriate for high-performance multi-functional applications and are also known as Functionally Graded Materials (FGMs). In continuous and discontinuous multi-material objects, the material composition or microstructure changes occur gradually and stepwise in one or more preferred directions. In discontinuous multi-material objects, the discontinuity at the interface of the material often leads to premature failure of the component because of the sudden differences in the mechanical properties. In contrast, the continuous multi-material objects show higher toughness and lower residual stress due to the change in the material and microstructure that occurs gradually (Kulkarni et al., 2021). Hence, continuous multi-material objects are widely used in aerospace, chemical, and other engineering fields. However, continuous multi-material objects are challenging to fabricate through WAAM as they require synergistic feeding of multiple wires into the melt pool to create the engineered alloys.

3 Different levels of hybridization in wire arc additive manufacturing

The hybridization of two processes brings out the strength of one to eliminate the limitation of another. In other words, different processes together can complement each other and make a better manufacturing system. The primary levels of

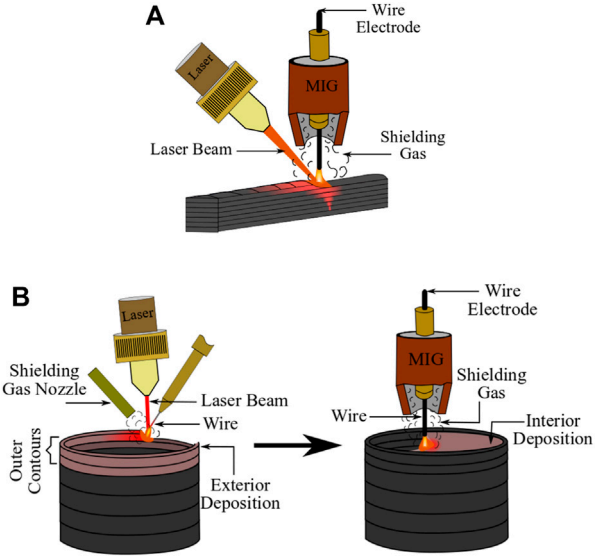

FIGURE 6
Laser-MIG hybrid-deposition **(A)** laser-assisted MIG deposition and **(B)** feature-based laser and MIG deposition.

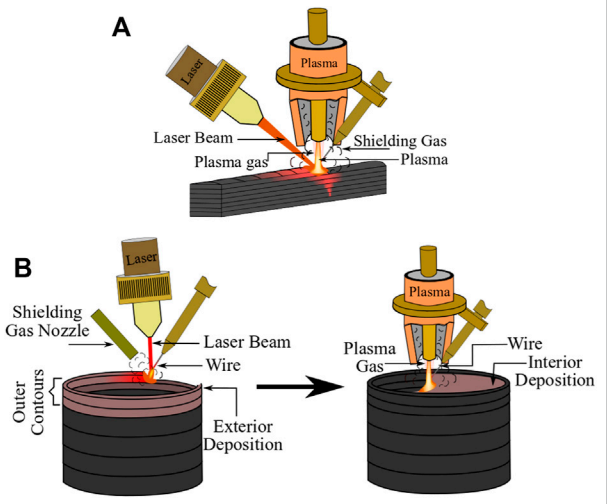

FIGURE 7
Laser-Plasma hybrid-deposition **(A)** laser-assisted TIG deposition and **(B)** feature-based laser and plasma deposition.

process hybridization, particularly in the WAAM process, are explained in the following sections.

3.1 Hybrid-deposition processes

This level of hybridization utilizes a hybrid Arc–welding technique to enhance the overall process capability, known as the "Hybrid-Deposition Process" Some of the feasible combinations of deposition processes are discussed in the following sections:

3.2 The metal inert gas-Laser hybrid-deposition

A MIG-laser hybrid-deposition process utilizes the benefits of Metal Inert Gas (MIG) welding and Laser welding. It can be achieved in two ways, viz., 1) laser-assisted MIG deposition and 2) feature-based laser and MIG deposition. A MIG deposition head deposits material in the first category, and a laser adds a secondary fusion energy source applied simultaneously at the same location. A low-power laser beam assists the build process, improves process stability, reduces spatter, and enhances the accuracy of the deposited bead (Pardal et al., 2019) (Zhang et al., 2018a). The schematic of the laser-assisted MIG deposition process is shown in Figure 6A. In the second category, MIG and laser deposition processes are selectively used for specific locations. The laser deposition can deposit precise beads but with a very low deposition rate; on the other hand, MIG deposition is capable of depositing material with a very high deposition rate with compromise in accuracy. Therefore, laser deposition can be used for precisely realizing the exterior boundaries of a layer, and MIG deposition can be used for realizing the interior of the layers. The schematic of this feature-based laser and MIG deposition is shown in Figure 6B.

3.3 Tungsten inert gas/plasma-laser hybrid-deposition

A TIG/plasma-laser hybrid-deposition method utilizes the benefits of TIG/plasma and Laser deposition processes. It can be achieved in two ways, viz., 1) laser-assisted TIG/plasma deposition and 2) feature-based laser and TIG/plasma deposition. In the first category, a TIG/plasma deposition head deposits material, and a laser adds a secondary fusion energy source applied simultaneously at the same location. A low-power laser beam assists the build process and improves process performance and part quality. The energy density of the plasma arc can be improved, and the plasma arc diameter favorably decreased, which enhances the accuracy of the part (Wang et al., 2014; Gong et al., 2020; Wang et al., 2021b). At the same time, arc igniting became easier because of plasma induced by the laser. With more energy, the depth of the melt pool increases, the microstructure improves, and the porosities decrease (Branco et al., 1999). The laser-assisted Plasma deposition process schematic is shown in Figure 7A; a similar representation can be extended for laser can TIG deposition. In the second category, TIG/plasma and laser deposition processes

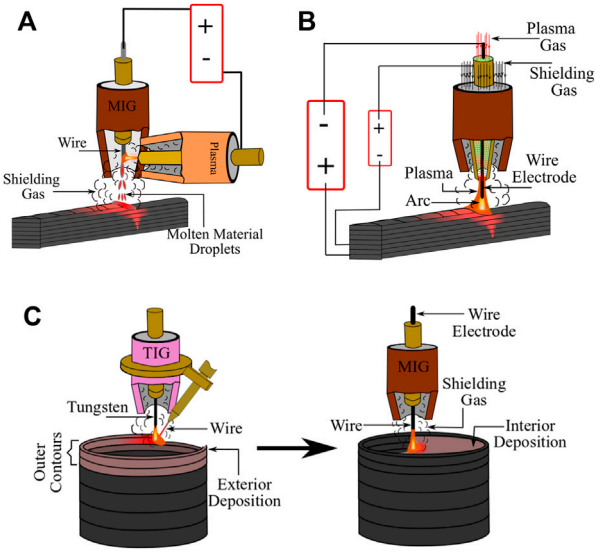

FIGURE 8
MIG-TIG/Plasma hybrid-deposition **(A)** plasma and MIG-based micro-casting, **(B)** plasma-assisted MIG deposition, and **(C)** Feature-based TIG and MIG deposition.

are selectively used for specific locations. The laser deposition can deposit precise beads but with a very low deposition rate; on the other hand, TIG/plasma deposition is capable of depositing material with a relatively high deposition rate with a relative compromisation in accuracy. Therefore, laser deposition can be used to precisely realize a layer's exterior boundaries, and TIG/plasma deposition can be used to realize the layers' interior. The schematic of this feature-based laser and plasma deposition is shown in Figure 7B; a similar representation can be extended for feature-based laser and TIG deposition.

3.4 Metal inert gas-tungsten inert gas/plasma hybrid-deposition

A MIG-TIG/plasma hybrid deposition utilizes the benefits of MIG and TIG/plasma deposition processes. It can be achieved in three ways, viz., 1) plasma and MIG-based micro-casting deposition, 2) plasma-assisted MIG deposition, and 3) feature-based TIG/Plasma and MIG deposition. Prinz and Weiss (Beck et al.), and Amon et al. (1998), proposed a plasma and MIG deposition-based micro-casting process for Shape Deposition Manufacturing (SDM). In this hybrid-deposition process, a plasma arc is established between the tungsten of a plasma deposition head and the wire of a MIG deposition head, as shown in Figure 8A. The wire melts in the plasma arc and accumulates the weight to further detach from its tip in the form of super-heated droplets. The droplet falls from the wire, accelerated by gravity, and flattens upon impact with the substrate. Ono et al. (2009) proposed a coaxial plasma-assisted MIG welding process to improve deposited beads and reduce spatter and fume generation, as shown in Figure 8B. This hybrid-deposition process is being implemented now in Additive Manufacturing (AM) to produce fully functional metallic objects. In the third category, MIG and TIG deposition processes are selectively used for specific locations. The TIG deposition can deposit precise beads but with a very low deposition rate; on the other hand, MIG deposition is capable of depositing material with a very high deposition rate with compromise in accuracy. Therefore, the TIG deposition can be used for precisely realizing the exterior boundaries of a layer, and MIG deposition can be used for realizing the interior of the layers. The schematic of this feature-based TIG and MIG deposition is shown in Figure 8C. By replacing TIG with Plasma deposition, a similar correlation can be extended for feature-based Plasma and MIG deposition. It can be noted that this hybridization will be cheaper than the feature-based laser and MIG deposition because of the low cost of TIG/plasma as compared to laser.

3.5 Hybrid-manufacturing processes

Owing to the differences between the type of arc (MIG/TIG/Plasma), in terms of precision/quality, speed, and cost, each energy source has its domain of applications. Several processes have been synergically hybridized with WAAM to overcome its limitation. In this context, arc welding with the milling process is the most common hybridization for layer consolidation. In this kind of hybrid-WAAM process, milling is used after the deposition of each layer to get the required layer thickness. After completion of the part, milling is also utilized for the final finishing of the part (Song et al., 2005; Karunakaran et al., 2010; Zhang et al., 2019b; Zhang et al., 2021b). In the studies by Song et al. (2005) apart from the surface finish and dimensional accuracy, a hybrid system of welding and milling was reported to fabricate parts with homogeneous microstructures with lower porosities, as shown in Figure 10E. The use of milling after each layer deposition can remove porosities, and coarser grains occur on the upper side of the layers (Prado-Cerqueira et al., 2017; Zhang et al., 2019b; Reisch et al., 2020). To understand residual stress generation in the WAAM, two models are generally used, viz., Thermal Gradient Model and the cool down phase model. In the case of the thermal gradient model, the inclusion of residual stress is caused by differential thermal expansion and contraction of the deposited metal and parent material. It has been reported that the nature of these residual stresses is tensile. In the cool down phase model, when the material is deposited over the substrate, it is in the molten state. The expansion of the deposited material generates compressive stress on the nearby area, as represented by the red color in Figure 9A. After a certain time, the deposited material starts to cool down and gets shrink; The

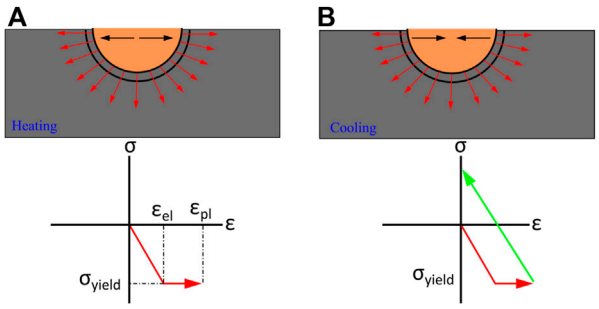

FIGURE 9
Residual stresses generated in substrate during cool down phase model during **(A)** heating and **(B)** cooling.

phenomenon leads to pulling its nearby material, and hence tensile stress is generated in the workpiece and is represented by the green color in Figure 9B. Finally, after completion of the process, tensile residual stresses remain in part. Compressive residual stresses are generally desirable as they result in high fatigue life of the manufactured objects.

Different processes are used combined with WAAM to provide compressive stress on the deposited layer, such as cold rolling (Hönnige et al., 2018), laser peening (Sun et al., 2018), vibrational peening (Yang et al., 2018), shot peening (Casarin et al., 2021), etc. The working principle of the different peening methods, along with cold rolling, are illustrated in Figures 10A–D. Furthermore, the impact of the different peening methods is listed in Table 1.

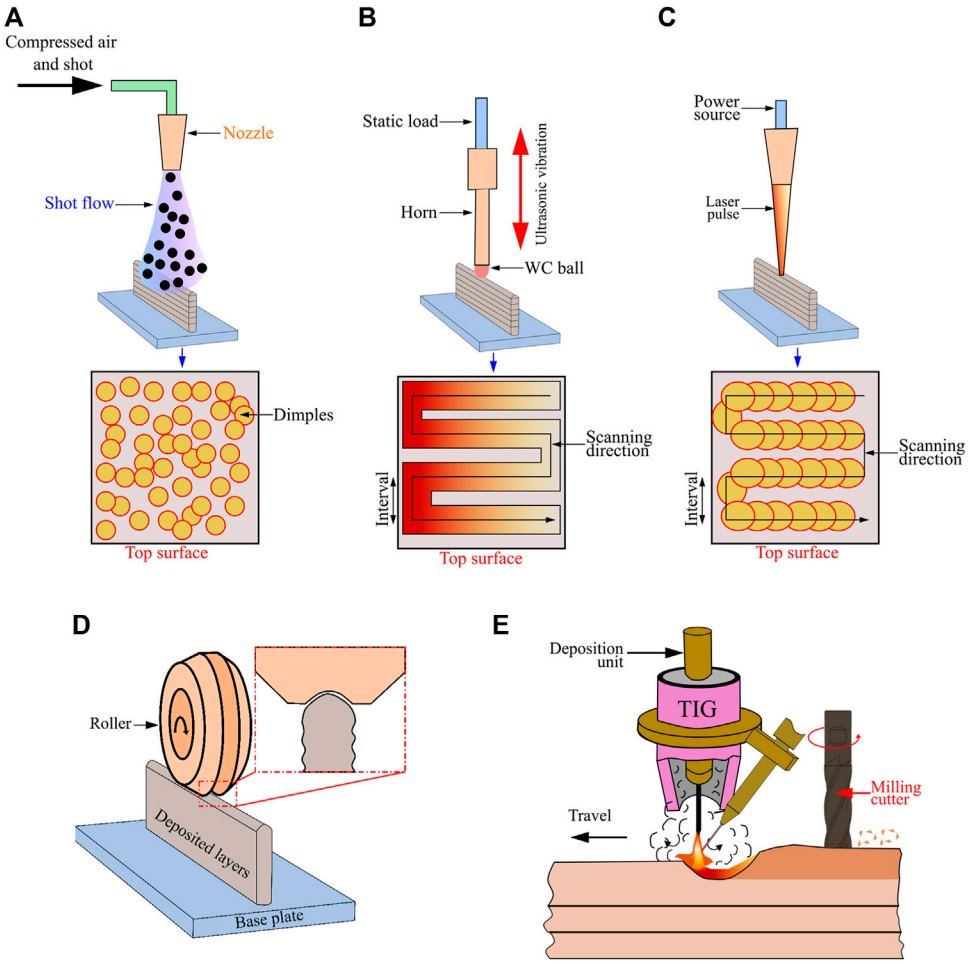

FIGURE 10
Peening **(A)** shot, **(B)** ultrasonic, **(C)** laser. **(D)** cold rolling, and **(E)** milling along with WAAM.

TABLE 1 Benefits associated with different post-processing techniques.

Material	Method	Benefits	References
Ti alloy (Ti-6Al-4V)	Shot peening	Fatigue life enhanced by 34%, with decreased short crack propagation rate by 34–60%	Wang et al. (2020c)
SS (304)	Shot peening	Increase of 52, 14, and 18% in the microhardness, strength, and fracture toughness	Tadge et al. (2015)
Mg alloy (AZ31)	Ultrasonic peening	141% enhancement in the microhardness with the reduced wear rate and improved coefficient of friction	Zhang et al. (2021c)
Al alloy (7075)	Ultrasonic peening	Reduced corrosion rate with refined grain structure	Pandey et al. (2017)
Duplex SS	Laser peening	74.2% reduction in corrosion rate with 39% reduction in wear volume	Lim et al. (2012)
SS (316L)	Laser peening	35% improvement in hardness with reduced corrosion rate	Ebrahimi et al. (2016)
Ti alloy (Ti-6Al-4V)	Cold rolling	A small grain of 0.62 μm with improved strength	Martina et al. (2013)
Al alloy (Al2325)	Milling + WAAM	Material utilization increased from 34 to 91%	Li et al. (2017)

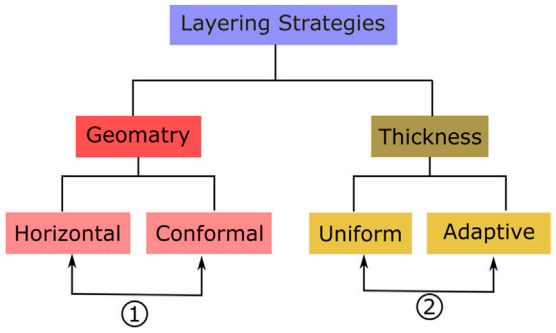

FIGURE 11
Hybrid-layering strategies.

3.6 Hybrid-layering strategies

It can be noted that WAAM cannot utilize a support structure to fabricate the overhanging/undercut features, and hence several layering strategies are developed over the period. In WAAM, a layer can be realized in two ways: 1) Horizontal or Conformal deposition and 2) Uniform or Adaptive layer thickness. These layering strategies are summarized in Figure 11. If two or more of these strategies are used to realize a component, it will be called a hybrid-layering strategy. Typically, parts fabricated by WAAM are horizontal deposition with uniformed layer thickness (Cunningham et al., 2018) (Kapil et al., 2020). However, using multi-axis kinematics for the motion has given scope for conformal deposition by WAAM.

3.7 Horizontal-conformal hybrid-layering strategy

Horizontal and conformal layering strategies are demonstrated for realizing a spherical object in Figures 12A,B, respectively. If an object is realized optimally using horizontal and conformal layering strategies, it is called a 'Horizontal-conformal hybrid-layering strategy. Usually, such hybrid-layering strategies are used to eliminate the need for a support mechanism; One can also use this hybridization to produce near-net shapes of the objects more accurately and efficiently with less staircase effect during deposition.

An example of the horizontal-conformal hybrid-layering strategy is shown in Figure 12C. In this illustrative example, "horizontal layers" produce the center part of the object, and "conformal layers" create an annular volume of the object on the periphery of the first volume. Many researchers have adopted this hybridization in the past (Alkadi et al., 2020; Sarma et al., 2021; Huang et al., 2022).

3.8 Uniform-adaptive hybrid-layering strategy

Adaptive layer thickness is a common strategy in AM to eliminate the need for a support mechanism and produce a more accurate near-net shape of the objects. However, optimal use of uniform and adaptive layers can save time and cost involved in manufacturing. An illustrative example of a uniform-adaptive hybrid-layering strategy for WAAM is shown in Figure 13. This object has been divided into two regions. There is no overhanging/undercut feature in Region-I; therefore, it can be realized using maximum uniform layer thickness. On the other hand, Region-II has an overhanging feature; hence it has to be realized by adaptive layer thickness to maintain constant overhang so that the support mechanism can be avoided.

The above-given example is for the horizontal layer; however, a similar analogy can be extended for a conformal uniform-adaptive hybrid-layering strategy. Hybrid layer strategies are primarily for enhancing the geometric capabilities and dimensional accuracy of WAAM and may not contribute significantly to eliminating the residual stresses.

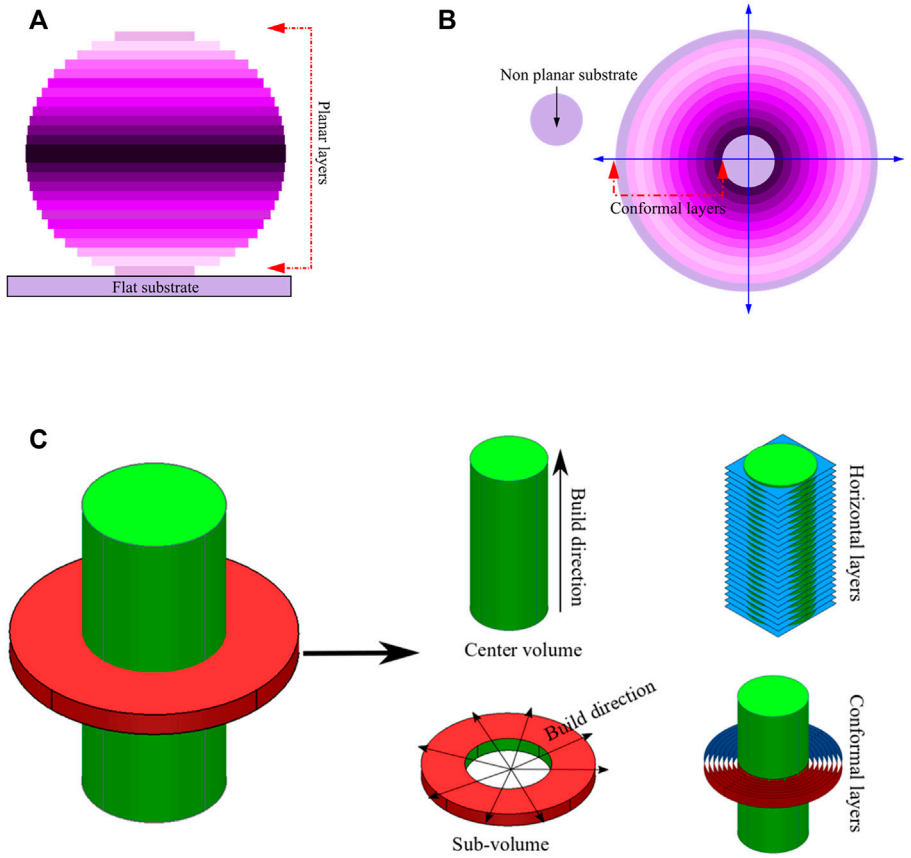

FIGURE 12
Layering strategies based on the geometry of the object **(A)** Horizontal, **(B)** Conformal, and **(C)** horizontal-conformal slicing.

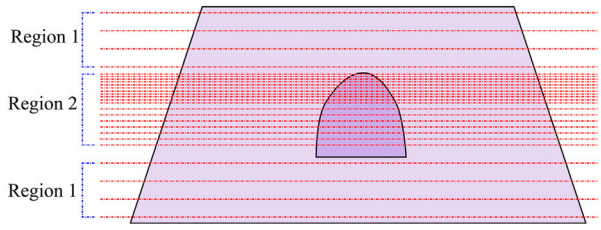

FIGURE 13
Uniform-adaptive hybrid-layering strategy.

3.9 Hybrid-machine tools

In the WAAM machine tool, multi-axis kinematics is required to eliminate the need for support material. The involvement of different kinematics makes the process more efficient and promising. Also, to add and remove the material optimally, a multi-axis machine tool is essential for WAAM. In a typical multi-axis machine tool, serial and parallel kinematics are two popular methods in the industry. In serial kinematics, every additional axis is mounted on the previous one, for example, a typical 5-axis CNC machine and robot arms. While in the case of parallel kinematics, several serial kinematic chains are used to support a single platform or end-effector. The most popular example of parallel kinematics is known as the Stewart Platform (Song et al., 2015). It has six linear actuators to move a platform in the desired position. Scissor lift is another example of parallel kinematics where two degrees of freedom can be achieved within a very compact area (Islam et al., 2014). In WAAM setup, CNC machines and robotics arms are popular for motion kinematics (Karunakaran et al., 2012; Bandari et al., 2015; Ding et al., 2015c; Prado-Cerqueira et al., 2017; Wu et al., 2017; Paskual et al., 2018). Robotic arms have better flexibility and work envelope with a compromisation in accuracy and stiffness. On the other hand, CNC machine tools can give microns of accuracy with higher stiffness. It is designed with massive structures and wide beds, which eliminates the flexibility that is significant in the case of robotic arms. Hybrid-machine tools such as a combination of serial and parallel kinematic or CNC and robotic arms utilize the

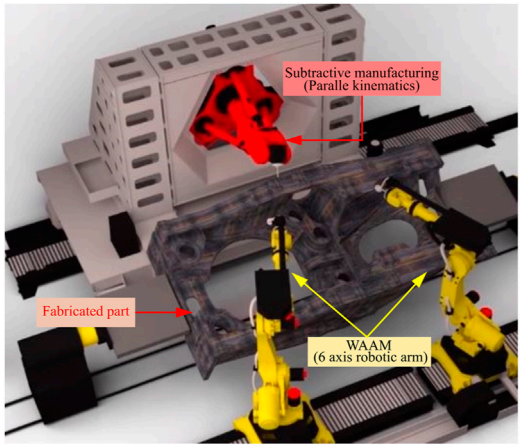

FIGURE 14
Uniform-adaptive hybrid-layering strategy Large Additive Subtractive Integrated Modular Machine.

advantages and eliminate the disadvantages, hence improving the process performance.

WAAM is the deposition technology utilized in LSIMM. It can be noted that LSIMM Large Additive Subtractive Integrated Modular Machine (LASIMM) is a hybrid WAAM system that utilizes two levels of hybridization, 1. Hybrid-manufacturing process (i.e., Additive + Subtractive) and 2. Hybrid-machine tool (i.e., the robotic arm (serial-kinematics) for deposition and Stewart platform (parallel-kinematics) for machining and inspection) as shown in Figure 14 (Assunção et al., 2018). Therefore, this system finds its application in realizing large and complicated metallic structures with significantly high dimensional accuracy.

3.10 Hybrid-raw stock

The hybrid-raw stock utilizes different materials during the deposition to fabricate high-performance multi-functional objects, also termed as Functionally Graded Materials (FGMs). It can be noted that it should be considered a hybrid-raw stock if using multiple raw stocks enhances the part quality, functionality, or process performance. A brief discussion on the utilization of hybrid-raw stock in WAAM is discussed in the subsequent section.

3.11 Hybrid-raw stock material

In this level of hybridization, two or more wires of different chemical compositions are used to fabricate high-performance multi-functional objects.

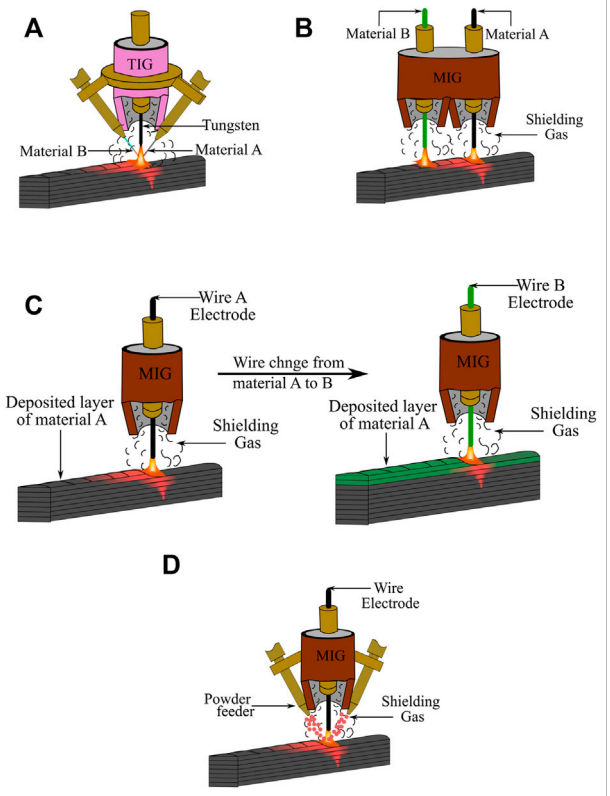

FIGURE 15
Hybrid-raw stock material in **(A)** TIG-WAAM, **(B)** tandem wire-based deposition system, **(C)** MIG-WAAM, and **(D)** hybrid-raw stock type in MIG-WAAM (powder + wire).

TIG-WAAM is widely preferred for the fabrication of high-performance multi-functional objects. In this process, multiple wires of different compositions can be simultaneously fed into the melt pool created by the arc (Yu et al., 2021). The federates of different wires can be varied to obtain a desirable spatial composition. As using multiple wires in WAAM can help realize components with varying metallurgical properties to improve the part's performance, this can be considered a level of hybridization in WAAM. Many researchers have fabricated such high-performance multi-functional objects using TIG-based WAAM (Busachi et al., 2015), (Gu et al., 2018), (Rodrigues et al., 2022), (Wang et al., 2018a), (Yu et al., 2021), (Dong et al., 2017), (Huang et al., 2020). The schematic of the TIG-based WAAM for fabricating multi-material objects is shown in Figure 15A.

MIG-WAAM is merely used to fabricate objects with continuously varying metallurgical properties due to the difficulty in synergistic integration between the secondary wire feeder and the MIG module. However, certain literature can be found on the realization of the objects with stepwise variation in metallurgical properties using MIG-WAAM (Chandrasekaran et al., 2020; Senthil et al., 2021; Ahsan et al., 2021; Rodrigues et al.,

TABLE 2 Features associated with different Hybrid-WAAM processes.

Hybrid-WAAM process	Features	References
WAAM + Milling	• Surface Roughness improves by 31.6% as compared to traditional WAAM. • A maximum of 93% reduction in surface residual stress can be achieved as compared to WAAM. • A maximum of 71.02% of material wastage can be minimized	(Zhang et al., 2019b; Zhang et al., 2021b; Sarma et al., 2022)
WAAM + Rolling	• Columnar dendrites change to finer equiaxed grains of 16.4 μm for Inconel 718 • 57% reduction in anisotropy coefficient as compared to traditional WAAM.	Zhang et al. (2022)
WAAM + Ultrasonic peening	• Around 50% reduction in grain diameter has been reported in the literature	Tian et al. (2021)
WAAM + Laser peening	• A maximum of 19% improvement in the hardness of the titanium alloy	Chi et al. (2020)
Steel + Copper	• The interface zone shows higher strength and elongation (690MPa and 16.6%) as compared to the copper only region • Reduction in the overall cost of the product • Gradual variation in mechanical properties such as microhardness (260HV to 120HV)	Rodrigues et al. (2022)
Stainless Steel + Inconel 625	• The gradual transition of microhardness (from 226HV to 272HV) demonstrates its application to two different wear environments • The produced FGM can be used in powerplant and nuclear water reactors • SS316L with Inconel 625 shows an 18% improvement in UTS as compared to pure SS.	(Mohan Kumar et al., 2021) (Sasikumar et al., 2022)
Aluminium + Titanium	• The oxidation reduction rate decreases with a decrease in aluminium content resulting this face exposure to a less oxidant environment • A gradual transition in hardness and tensile strength can be observed in the component along the build direction	Wang et al. (2018a)
LCS + SS	• 124% improvement on average hardness on the LCS side • Tensile strength has been observed to be increased by 46 and 40% as compared to LCS and SS respectively	Yu et al. (2021)
Raw stock	• A maximum of 9.5 kg/h deposition rate can be achieved	Busachi et al. (2015)
Robot + CNC	• Improved accuracy and reduced cost of production • Larger work envelop can be achieved with a hybrid robot + CNC setup	(Bandari et al., 2015) (Freire et al., 2020)
Conformal + Horizontal	• A maximum error of ± 1.6 mm has been reported in the literature • Better dimensional accuracy and surface finish are obtained as compared to horizontal slicing • Issues such as staircase error can be avoided, along with improved material bonding in the curvature	(Authora) (Shembekar et al., 2019)
Uniform + Adaptive	• Significant reduction in built time and staircase effect • etter geometrical accuracy and part performance have been reported in literature	(Zhao and Guo, 2020) (Sarma et al., 2021)
Adaptive + Conformal	• Adaptive slicing yields reduced built time, while conformal slicing results in better geometrical accuracy leading to reduction in built time	Panchagnula and Simhambhatla, (2016)
Laser + GMAW	• 20% improvement in surface roughness • 34% improvement in the elongation along with reduced anisotropy. The yield strength has been reported to be enhanced by 15% • The content of bad {001} <100 > -cube texture was reduced by 11.8% as compared to pure WAAM.	Gong et al. (2020)
Laser + GTAW	• The UTS and YS is enhanced by 11.4 and 29.9% as compared to WAAM. • Significant reduction in residual stress • The small angle grain boundary is reduced by 70% in the case of Hybrid Laser-based WAAM. • Refined grains and improved nanoscale precipitates lead to improvement in mechanical properties	(Liu et al., 2022) (Ma et al., 2022)
GMAW + GTAW	• An improvement of 20% in UTS and 17% improvement in hardness as compared to traditional WAAM • Significant reduction in heat input resulting in reduced warpage of the substrate	Zhou et al. (2022)

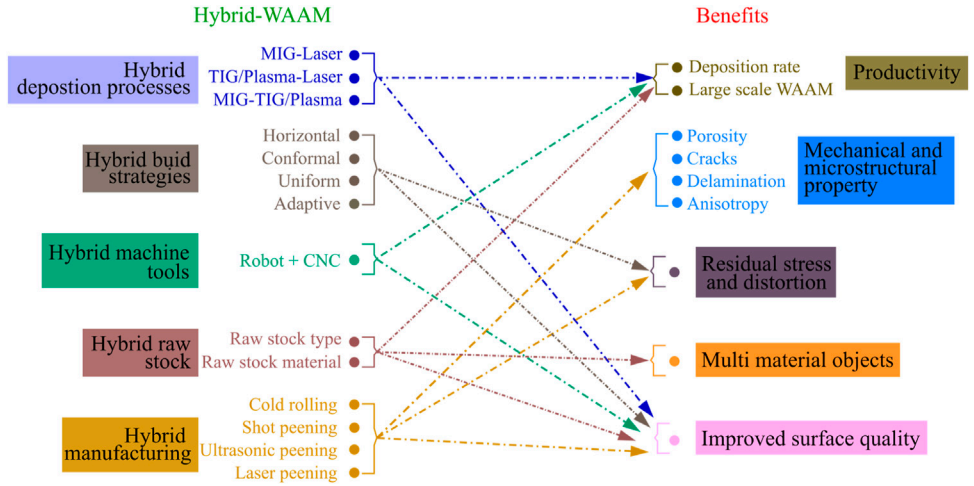

FIGURE 16
Benefits associated with different hybrid-WAAM methods.

2021; Rodrigues et al., 2022). In this level of hybridization, the first few layers are deposited using one material, followed by depositing the subsequent layers of another material, as shown in Figure 15C. Chandrasekaran et al. (2022) have used MIG-WAAM to fabricate marine risers that can sustain the high-temperature environment. The build time in this process is inherently high due to the requirement of changing feedstock wire during deposition. However, this issue can be overcome by adopting a tandem wire-based MIG-WAAM (Gu et al., 2018), (Adinarayanappa and Simhambhatla, 2015). This will also help in fabricating continuous bimetallic objects. The schematic representation of the process is illustrated in Figure 15B.

3.12 Hybrid-raw stock type

Wires and powders as raw stock are widely used in metal-AM; the former is cost-effective and produces parts with high material integrity, while the latter is flexible to use and produces parts with better accuracy (Paskual et al., 2018) (Karunakaran et al., 2012). Hybridization between two can utilize the advantages of both and eliminate the disadvantages. Therefore, this level of hybridization is known as hybrid-raw stock type and has been explored by researchers to fabricate high-performance multi-functional objects. Sun et al. (2022) developed Wire Arc Powder Additive Manufacturing (WAP-AM) system, as shown in Figure 15D; The ceramic particles are injected into the melt pool of the aluminum to fabricate Aluminium Matrix Composite (AMC) structures. As a class of advanced structural materials, AMC is suitable for industrial applications because of its low densities, high specific strengths, good thermal conductivities, and high wear resistance (Surappa, 2003).

Furthermore, apart from these hybrid technologies, the defects can also be reduced through the wire feed and its oscillation which is discussed in the next section.

3.13 Wire feed and its oscillation

The property of the fabricated parts can be further improved by applying certain *in situ* oscillation-based processes. These processes yield the disintegration of dendrites from the mushy zone of the weld pool due to the weld pool stirring effect (Kou, 2002). Since these particles are swept into the center of the melt pool, nucleation is initiated from these sites only. This also helps in obtaining refined microstructures due to increased stirring within the melt pool (Biradar and Raman, 2012; Hua et al., 2017; Wang and Xue, 2017). The crack resistance and surface roughness were found to be increased for nickel-based filler metal (Wu and Kovacevic, 2005) (Yu et al., 2014). Moreover, other materials such as magnesium alloy, aluminum, low carbon steel, titanium alloy, stainless steel, etc. There are broadly two methods for the generation of oscillations in the melt pool: 1) Torch-based oscillation, 2) wire feeder-based oscillation, and 3) workpiece-based oscillation. The first one can be achieved through modulation of power supply, shielding gas modulation, and weld torch and electrode oscillations. The power supply modulation helps in achieving different current zones for arc stability and material detachment. This, in turn, reduces the cooling rate of the molten metal resulting formation of different phases. Power supply modulation generally involves

pulse waveform, double pulse waveform, variable polarity, and double pulse method (Wang et al., 2018b).

The composition of shielding gas has a significant effect on the geometry of the arc. The transition from argon to CO2 results in a constricted arc. This yields a strong stirring of the melt pool. The refinement in the grain and improved ductility in the case of GTAW-based WAAM of Al 6061 has been reported in the literature due to weld torch vibration with an amplitude of 1.4 mm. The basic method of wire feeder-based oscillation involves ultrasonic wire oscillation. The improvement in mechanical properties and stable and rapid droplet transfer has been claimed in literature (Watanabe et al., 2010). The cold metal transfer-based GMAW method combines pulse and wire oscillation to synchronize the short circuit-based metal transfer. This process has been proved to yield higher hardness and better geometrical accuracy as compared to traditional GMAW (Wu and Kovacevic, 2005) (Queguineur et al., 2018) (Zhang et al., 2018b). Similarly, it is also possible to oscillate the substrate with the help of an external force (Wen et al., 2015) (Yuan et al., 2016b). However, this method is limited to small-scaled WAAM fabricated components. Likewise, an electromagnetic force-based direct stirring of the weld pool can also be observed in the literature. (Zhang et al., 2019a). The aforementioned methods help in eliminating the defects such as columnar grains, porosity, surface roughness, etc. resulting significant improvement in the mechanical and geometrical properties.

4 Conclusion

To compete with traditional manufacturing technologies and comply with the qualifying requirements for industrial applications, Wire Arc Additive Manufacturing (WAAM) should be able to produce fully functional and defect-free parts with a significantly high deposition rate. Hybridization in WAAM systems can produce parts free from residual stresses, porosities, anisotropies, and cracks while maintaining a high deposition rate and an excellent dimensional accuracy. The benefits of the hybrid-WAAM increase its demand in the manufacturing sector with an enormous scope of material that can be fabricated.

This paper takes readers on a journey that starts with the history, classification, and working principles of WAAM and ends with an overview of the hybrid-WAAM developed in the last decade. This paper proposed different levels of hybridization in WAAM, viz., hybrid-deposition processes, hybrid-manufacturing processes, hybrid-layering strategies, hybrid-machine tools, and hybrid-raw stock. The authors' unique perspectives are some of these levels of hybridization in WAAM. However, it can be noted that any of the proposed levels of hybridization in WAAM are intended to be fully coupled, synergetic, and improve the part's functionality and process performance. This paper will help the reader identify a particular level of hybridization in WAAM based on their objectives. For example, the hybrid deposition processes must be targeted to increase the deposition rate. The features associated with the different Hybrid-WAAM processes are listed in Table 2. Furthermore, the benefits associated with proposed different levels of a hybrid-WAAM are summarized in Figure 16.

Author contributions

SK conceptualized, collected the data, and wrote the paper, AR collected the data and wrote the paper, and RS collected the data and wrote the paper.

Conflict of interest

The authors declare that the research was conducted in the absence of any commercial or financial relationships that could be construed as a potential conflict of interest.

Publisher's note

Acknowledgments

We acknowledge Indo-German Science and Technology Centre (IGSTC) for theirfinancial support for project No. IGSTC/Call 2020/MAMM-WAAM/50/2021-22/259 entitled "Multi-Axis Multi-material Wire Arc Additive Manufacturing (MAMM-WAAM)".

References

Adinarayanappa, S. M., and Simhambhatla, S. (2015). Determination of Process Parameter for Twin-Wire Weld-Deposition Based Additive Manufacturing. *Proc. ASME Des. Eng. Tech. Conf.* 4. doi:10.1115/DETC2014-34658

Ahsan, M. R. U., Fan, X., Seo, G. J., Ji, C., Noakes, M., Nycz, A., et al. (2021). Microstructures and Mechanical Behavior of the Bimetallic Additively-Manufactured Structure (BAMS) of Austenitic Stainless Steel and Inconel 625. *J. Mater Sci. Technol.* 74, 176–188. doi:10.1016/J.JMST.2020.10.001

Ahsan, M. R. U., Tanvir, A. N. M., Seo, G. J., Bates, B., Hawkins, W., Lee, C., et al. (2020). Heat-treatment Effects on a Bimetallic Additively-Manufactured Structure (BAMS) of the Low-Carbon Steel and Austenitic-

Stainless Steel. *Addit. Manuf.* 32, 101036. doi:10.1016/J.ADDMA.2020.101036

Alkadi, F., Lee, K. C., Bashiri, A. H., and Choi, J. W. (2020). Conformal Additive Manufacturing Using a Direct-Print Process. *Addit. Manuf.* 32, 100975. doi:10.1016/J.ADDMA.2019.100975

Amon, C. H., Beuth, J. L., Weiss, L. E., Merz, R., and Prinz, F. B. (1998). Shape Deposition Manufacturing with Microcasting: Processing, Thermal and Mechanical Issues. *J. Manuf. Sci. Eng.* 120, 656–665. doi:10.1115/1.2830171

Arita, H., Morimoto, T., Nagaoka, S., and Nakano, T. (20092013). Development of Advanced 3-Electrode MAG High-Speed Horizontal Fillet Welding Process. *Weld. World* 53, 35–43. doi:10.1007/BF03266713

Artaza, T., Bhujangrao, T., Suárez, A., Veiga, F., and Lamikiz, A. (2020). Influence of Heat Input on the Formation of Laves Phases and Hot Cracking in Plasma Arc Welding (PAW) Additive Manufacturing of Inconel 718. *Met* 10, 771. doi:10.3390/MET10060771

Artaza, T., Suárez, A., Murua, M., García, J. C., Tabernero, I., and Lamikiz, A. (2019). Wire Arc Additive Manufacturing of Mn4Ni2CrMo Steel: Comparison of Mechanical and Metallographic Properties of PAW and GMAW. *Procedia Manuf.* 41, 1071–1078. doi:10.1016/J.PROMFG.2019.10.035

Artaza, T., Suárez, A., Veiga, F., Braceras, I., Tabernero, I., Larrañaga, O., et al. (2020). Wire Arc Additive Manufacturing Ti6Al4V Aeronautical Parts Using Plasma Arc Welding: Analysis of Heat-Treatment Processes in Different Atmospheres. *J. Mater Res. Technol.* 9, 15454–15466. doi:10.1016/J.JMRT.2020.11.012

Assunção, E., Quintino, L., Martina, F., Williams, S., Pires, I., and Lopez, A. (2018). *LASIMM-AM Production of Large Scale Engineering Structures*.

Bai, X., Colegrove, P., Ding, J., Zhou, X., Diao, C., Bridgeman, P., et al. (2018). Numerical Analysis of Heat Transfer and Fluid Flow in Multilayer Deposition of PAW-Based Wire and Arc Additive Manufacturing. *Int. J. Heat. Mass Transf.* 124, 504–516. doi:10.1016/J.IJHEATMASSTRANSFER.2018.03.085

Baker, R. (1925). *Method of Making Decorative Articles. US1533300A*. Pennsylvania: U.S. Patent and Trademark Office.

Bandari, Y., Williams, S., Ding, J., and Martina, F. (2015). "Additive manufacture of large structures: robotic or CNC systems," in *2014 International Solid Freeform Fabrication Symposium*. (University of Texas at Austin).

Biradar, N. S., and Raman, R. (2012). Grain Refinement in Al-Mg-Si Alloy TIG Welds Using Transverse Mechanical Arc Oscillation. *J. Mater Eng. Perform.* 21, 2495–2502. doi:10.1007/S11665-012-0207-2/FIGURES/10

Branco, C. M., Maddox, S. J., Infante, V., and Gomes, E. C. (1999). Fatigue Performance of Tungsten Inert Gas (TIG) and Plasma Welds in Thin Sections. *Int. J. Fatigue* 21, 587–601. doi:10.1016/S0142-1123(98)00084-X

Busachi, A., Erkoyuncu, J., Colegrove, P., Martina, F., and Ding, J. (2015). Designing a WAAM Based Manufacturing System for Defence Applications. *Procedia CIRP* 37, 48–53. doi:10.1016/J.PROCIR.2015.08.085

Casarin, S. J., De Angelo Sanchez, L. E., Bianchi, E. C., Scalon, V. L., Fragelli, R. L., De Godoi, E. L., et al. (2021). *Effect of Burnishing on Inconel 718 Workpiece Surface Heated by Infrared Radiation*, 36, 1853–1864. doi:10.1080/10426914.2021.1926494

Chandrasekaran, S., Hari, S., and Amirthalingam, M. (2022). Functionally Graded Materials for Marine Risers by Additive Manufacturing for High-Temperature Applications: Experimental Investigations. *Structures* 35, 931–938. doi:10.1016/J.ISTRUC.2021.12.004

Chandrasekaran, S., Hari, S., and Amirthalingam, M. (2020). Wire Arc Additive Manufacturing of Functionally Graded Material for Marine Risers. *Mater Sci. Eng. A* 792, 139530. doi:10.1016/J.MSEA.2020.139530

Chi, J., Cai, Z., Wan, Z., Zhang, H., Chen, Z., Li, L., et al. (2020). Effects of Heat Treatment Combined with Laser Shock Peening on Wire and Arc Additive Manufactured Ti17 Titanium Alloy: Microstructures, Residual Stress and Mechanical Properties. *Surf. Coatings Technol.* 396, 125908. doi:10.1016/J.SURFCOAT.2020.125908

Colegrove, P. A., Coules, H. E., Fairman, J., Martina, F., Kashoob, T., Mamash, H., et al. (2013). Microstructure and Residual Stress Improvement in Wire and Arc Additively Manufactured Parts through High-Pressure Rolling. *J. Mater Process Technol.* 213, 1782–1791. doi:10.1016/J.JMATPROTEC.2013.04.012

Cong, B., Ding, J., and Williams, S. (20142014). Effect of Arc Mode in Cold Metal Transfer Process on Porosity of Additively Manufactured Al-6.3%Cu Alloy. *Int. J. Adv. Manuf. Technol.* 76, 1593–1606. doi:10.1007/S00170-014-6346-X

Cunningham, C. R., Flynn, J. M., Shokrani, A., Dhokia, V., and Newman, S. T. (2018). Invited Review Article: Strategies and Processes for High Quality Wire Arc Additive Manufacturing. *Addit. Manuf.* 22, 672–686. doi:10.1016/J.ADDMA.2018.06.020

Davis, T. A. (2004). The Effect of Process Parameters on Laser-Deposited TI-6A1-4V. *Electron Theses Diss.* doi:10.18297/etd/319

Derekar, K. S. (2018). *A Review of Wire Arc Additive Manufacturing and Advances in Wire Arc Additive Manufacturing of Aluminium*, 34, 895. doi:10.1080/02670836.2018.1455012

Derekar, K. S., Addison, A., Joshi, S. S., Zhang, X., Lawrence, J., Xu, L., et al. (2020). Effect of Pulsed Metal Inert Gas (Pulsed-MIG) and Cold Metal Transfer (CMT) Techniques on Hydrogen Dissolution in Wire Arc Additive Manufacturing (WAAM) of Aluminium. *Int. J. Adv. Manuf. Technol.* 107, 311–331. doi:10.1007/S00170-020-04946-2/TABLES/11

Ding, D., Pan, Z., Cuiuri, D., and Li, H. (2015). A Multi-Bead Overlapping Model for Robotic Wire and Arc Additive Manufacturing (WAAM). *Robot. Comput. Integr. Manuf.* 31, 101–110. doi:10.1016/J.RCIM.2014.08.008

Ding, D., Pan, Z., Cuiuri, D., and Li, H. (2015). "Process Planning for Robotic Wire and Arc Additive Manufacturing," in Proc 2015 10th IEEE Conf Ind Electron Appl ICIEA, 2000–2003. doi:10.1109/ICIEA.2015.7334441

Dinovitzer, M., Chen, X., Laliberte, J., Huang, X., and Frei, H. (2019). Effect of Wire and Arc Additive Manufacturing (WAAM) Process Parameters on Bead Geometry and Microstructure. *Addit. Manuf.* 26, 138–146. doi:10.1016/J.ADDMA.2018.12.013

Dong, B., Pan, Z., Shen, C., Ma, Y., and Li, H. (2017). Fabrication of Copper-Rich Cu-Al Alloy Using the Wire-Arc Additive Manufacturing Process. *Metall. Mater Trans. B Process Metall. Mater Process Sci.* 48, 3143–3151. doi:10.1007/S11663-017-1071-0/FIGURES/7

Ebrahimi, M., Amini, S., and Mahdavi, S. M. (20162016). The Investigation of Laser Shock Peening Effects on Corrosion and Hardness Properties of ANSI 316L Stainless Steel. *Int. J. Adv. Manuf. Technol.* 88, 1557–1565. doi:10.1007/S00170-016-8873-0

Fang, X., Zhang, L., Chen, G., Dang, X., Huang, K., Wang, L., et al. (2018). Correlations between Microstructure Characteristics and Mechanical Properties in 5183 Aluminium Alloy Fabricated by Wire-Arc Additive Manufacturing with Different Arc Modes. *Mater* 11, 2075. doi:10.3390/MA11112075

Freire, B., Babcinschi, M., Ferreira, L., Señaris, B., Vidal, F., and Neto, P. (2020). Direct Energy Deposition: a Complete Workflow for the Additive Manufacturing of Complex Shape Parts. *Procedia Manuf.* 51, 671–677. doi:10.1016/J.PROMFG.2020.10.094

Fu, R., Tang, S., Lu, J., Cui, Y., Li, Z., Zhang, H., et al. (2021). Hot-wire Arc Additive Manufacturing of Aluminum Alloy with Reduced Porosity and High Deposition Rate. *Mater Des.* 199, 109370. doi:10.1016/J.MATDES.2020.109370

Geng, H., Li, J., Xiong, J., Lin, X., and Zhang, F. (2017). Optimization of Wire Feed for GTAW Based Additive Manufacturing. *J. Mater Process Technol.* 243, 40–47. doi:10.1016/J.JMATPROTEC.2016.11.027

Gong, M., Meng, Y., Zhang, S., Zhang, Y., Zeng, X., and Gao, M. (2020). Laser-arc Hybrid Additive Manufacturing of Stainless Steel with Beam Oscillation. *Addit. Manuf.* 33, 101180. doi:10.1016/J.ADDMA.2020.101180

Gu, J., Bai, J., Ding, J., Williams, S., Wang, L., and Liu, K. (2018). Design and Cracking Susceptibility of Additively Manufactured Al-Cu-Mg Alloys with Tandem Wires and Pulsed Arc. *J. Mater Process Technol.* 262, 210–220. doi:10.1016/J.JMATPROTEC.2018.06.030

Gu, J., Jialuo, D., Stewart W., W., Huimin, G., Jing, B., Zhai, Y., et al. (2016). The strengthening effect of inter-layer cold working and post-deposition heat treatment on the additively manufactured Al-6.3 Cu alloy. *Mater. Sci. Eng.* 651, 18–26.

Guo, Y., Han, Q., Hu, J., Yang, X., Mao, P., Wang, J., et al. (2022). Comparative Study on Wire-Arc Additive Manufacturing and Conventional Casting of Al–Si Alloys: Porosity, Microstructure and Mechanical Property. *Acta Metall. Sin. Engl. Lett.* 35, 475–485. doi:10.1007/S40195-021-01314-1/FIGURES/9

Hauser, T., Reisch, R. T., Breese, P. P., Lutz, B. S., Pantano, M., Nalam, Y., et al. (2021). Porosity in Wire Arc Additive Manufacturing of Aluminium Alloys. *Addit. Manuf.* 41, 101993. doi:10.1016/J.ADDMA.2021.101993

Hönnige, J. R., Colegrove, P. A., Ganguly, S., Eimer, E., Kabra, S., and Williams, S. (2018). Control of Residual Stress and Distortion in Aluminium Wire + Arc Additive Manufacture with Rolling. *Addit. Manuf.* 22, 775–783. doi:10.1016/J.ADDMA.2018.06.015

Hua, C., Lu, H., Yu, C., Chen, J. M., Wei, X., and Xu, J. J. (2017). Reduction of Ductility-Dip Cracking Susceptibility by Ultrasonic-Assisted GTAW. *J. Mater Process Technol.* 239, 240–250. doi:10.1016/J.JMATPROTEC.2016.08.018

Huang, H., Ma, N., Chen, J., Feng, Z., and Murakawa, H. (2020). Toward Large-Scale Simulation of Residual Stress and Distortion in Wire and Arc Additive Manufacturing. *Addit. Manuf.* 34, 101248. doi:10.1016/J.ADDMA.2020.101248

Huang, J., Qin, Q., Wen, C., Chen, Z., Huang, K., Fang, X., et al. (2022). A Dynamic Slicing Algorithm for Conformal Additive Manufacturing. *Addit. Manuf.* 51, 102622. doi:10.1016/J.ADDMA.2022.102622

Islam, M. T., Yin, C., Jian, S., and Rolland, L. (2014). "Dynamic Analysis of Scissor Lift Mechanism through Bond Graph Modeling," in IEEE/ASME Int Conf Adv Intell Mechatronics, AIM, 1393–1399. doi:10.1109/AIM.2014.6878277

Jafari, D., Vaneker, T. H. J., and Gibson, I. (2021). Wire and Arc Additive Manufacturing: Opportunities and Challenges to Control the Quality and Accuracy of Manufactured Parts. *Mater Des.* 202, 109471. doi:10.1016/J.MATDES.2021.109471

Kapil, S., Negi, S., Joshi, P., Sonwane, J., Sharma, A., Bhagchandani, R., and Karunakaran, K. P. (2017). 5-Axis Slicing Methods for Additive Manufacturing Process. International Solid Freeform Fabrication Symposium.

Kapil, S., Joshi, P., Kulkarni, P. M., Negi, S., Kumar, R., and Karunakaran, K. P. (2018a). Elimination of Support Mechanism in Additive Manufacturing through Substrate Tilting. *Rapid Prototyp. J.* 24, 1155–1165. doi:10.1108/RPJ-07-2017-0139/FULL/PDF

Kapil, S., Kulkarni, P., Joshi, P., Negi, S., and Karunakaran, K. P. (2018b). *Retrofitment of a CNC Machine for Omni-Directional Tungsten Inert Gas Cladding*. 293–306. doi:10.1080/17452759.2018.1552484

Kapil, S., Legesse, F., Negi, S., Karunakaran, K. P., and Bag, S. (2020). Hybrid Layered Manufacturing of a Bimetallic Injection Mold of P20 Tool Steel and Mild Steel with Conformal Cooling Channels. *Prog. Addit. Manuf.* 5, 183–198. doi:10.1007/S40964-020-00129-3/TABLES/10

Karunakaran, K. P., Bernard, A., Suryakumar, S., Dembinski, L., and Taillandier, G. (2012). Rapid Manufacturing of Metallic Objects. *Rapid Prototyp. J.* 18, 264–280. doi:10.1108/13552541211231644/FULL/PDF

Karunakaran, K. P., Suryakumar, S., Pushpa, V., and Akula, S. (2010). Low Cost Integration of Additive and Subtractive Processes for Hybrid Layered Manufacturing. *Robot. Comput. Integr. Manuf.* 26, 490–499. doi:10.1016/J.RCIM.2010.03.008

Kim, J. Y., Lee, D. Y., Lee, J., and Lee, S. H. (2021). Parameter Optimization of Hybrid-Tandem Gas Metal Arc Welding Using Analysis of Variance-Based Gaussian Process Regression. *Met* 11, 1087. doi:10.3390/MET11071087

Kou, S. (2002). Welding Metallurgy. *Weld. Metall.* doi:10.1002/0471434027

Kozamernik, N., Bračun, D., and Klobčar, D. (2020). WAAM System with Interpass Temperature Control and Forced Cooling for Near-Net-Shape Printing of Small Metal Components. *Int. J. Adv. Manuf. Technol.* 110, 1955–1968. doi:10.1007/S00170-020-05958-8/FIGURES/17

Kulkarni, J. D., Goka, S. B., Parchuri, P. K., Yamamoto, H., Ito, K., and Simhambhatla, S. (2021). Microstructure Evolution along Build Direction for Thin-Wall Components Fabricated with Wire-Direct Energy Deposition. *Rapid Prototyp. J.* 27, 1289–1301. doi:10.1108/RPJ-04-2020-0085/FULL/PDF

Li, F., Chen, S., Shi, J., Tian, H., and Zhao, Y. (2017). Evaluation and Optimization of a Hybrid Manufacturing Process Combining Wire Arc Additive Manufacturing with Milling for the Fabrication of Stiffened Panels. *Appl. Sci.* 7, 1233. doi:10.3390/APP7121233

Li, Z., Liu, C., Xu, T., Ji, L., Wang, D., Lu, J., et al. (2019). Reducing Arc Heat Input and Obtaining Equiaxed Grains by Hot-Wire Method during Arc Additive Manufacturing Titanium Alloy. *Mater Sci. Eng. A* 742, 287–294. doi:10.1016/J.MSEA.2018.11.022

Lim, H., Kim, P., Jeong, H., and Jeong, S. (2012). Enhancement of Abrasion and Corrosion Resistance of Duplex Stainless Steel by Laser Shock Peening. *J. Mater Process Technol.* 212, 1347–1354. doi:10.1016/J.JMATPROTEC.2012.01.023

Liu, D., Wu, D., Wang, R., Shi, J., Niu, F., and Ma, G. (2022). Formation Mechanism of Al-Zn-Mg-Cu Alloy Fabricated by Laser-Arc Hybrid Additive Manufacturing: Microstructure Evaluation and Mechanical Properties. *Addit. Manuf.* 50, 102554. doi:10.1016/J.ADDMA.2021.102554

Liu, H. H., Zhao, T., Li, L. Y., Liu, W. J., Wang, T. Q., and Yue, J. F. (2020). A path planning and sharp corner correction strategy for wire and arc additive manufacturing of solid components with polygonal cross-sections. *Int. J. Adv. Manuf. Technol.* 106 (11), 4879–4889.

Ma, G., Wu, S., Wang, R., Liu, D., Niu, F., Bi, G., et al. (2022). Microstructure Evaluation and Resultant Mechanical Properties of Laser- Arc Hybrid Additive Manufactured Cu-Cr-Zr Alloy. *J. Alloys Compd.* 912, 165044. doi:10.1016/J.JALLCOM.2022.165044

Marinelli, G., Martina, F., Ganguly, S., and Williams, S. (2019). Development of Wire + Arc Additive Manufacture for the Production of Large-Scale Unalloyed Tungsten Components. *Int. J. Refract Met. Hard Mater* 82, 329–335. doi:10.1016/J.IJRMHM.2019.05.009

Martina, Filomeno, Williams, Stewart W., and Colegrove, P. (2013). Improved Microstructure and Increased Mechanical Properties. *Sff Sumpos.*, 490–496.

Mohan Kumar, S., Rajesh Kannan, A., Pravin Kumar, N., Pramod, R., Siva Shanmugam, N., Vishnu, A. S., et al. (2021). Microstructural Features and Mechanical Integrity of Wire Arc Additive Manufactured SS321/Inconel 625 Functionally Gradient Material. *J. Mater Eng. Perform.* 30, 5692–5703. doi:10.1007/S11665-021-05617-3/FIGURES/13

Negi, S., Kapil, S., Sharma, A., Choudhary, P., Bhargava, P., and Karunakaran, K. P. (2020). *Retrofitment of Laser Cladding System with CNC Machine for Hybrid Layer Manufacturing*, 47–59. doi:10.1007/978-981-32-9433-2_4

Nilsiam, Y., Sanders, P., and Pearce, J. M. (2017). Slicer and Process Improvements for Open-Source GMAW-Based Metal 3-D Printing. *Addit. Manuf.* 18, 110–120. doi:10.1016/J.ADDMA.2017.10.007

Ning, F., and Cong, W. (2016). Microstructures and Mechanical Properties of Fe-Cr Stainless Steel Parts Fabricated by Ultrasonic Vibration-Assisted Laser Engineered Net Shaping Process. *Mater Lett.* 179, 61–64. doi:10.1016/J.MATLET.2016.05.055

Ono, K., Liu, Z., Era, T., Uezono, T., Ueyama, T., Tanaka, M., et al. (2009). *Development of a Plasma MIG Welding System for Aluminium*, 23, 805–809. doi:10.1080/09507110902836945

Panchagnula, J. S., and Simhambhatla, S. (2016). *Inclined Slicing and Weld-Deposition for Additive Manufacturing of Metallic Objects with Large Overhangs Using Higher Order Kinematics*, 11, 99–108. doi:10.1080/17452759.2016.1163766

Pandey, V., Singh, J. K., Chattopadhyay, K., Srinivas, N. C. S., and Singh, V. (2017). Influence of Ultrasonic Shot Peening on Corrosion Behavior of 7075 Aluminum Alloy. *J. Alloys Compd.* 723, 826–840. doi:10.1016/J.JALLCOM.2017.06.310

Pardal, G., Martina, F., and Williams, S. (2019). Laser Stabilization of GMAW Additive Manufacturing of Ti-6Al-4V Components. *J. Mater Process Technol.* 272, 1–8. doi:10.1016/J.JMATPROTEC.2019.04.036

Paskual, A., Álvarez, P., and Suárez, A. (2018). Study on arc welding processes for high deposition rate additive manufacturing. *Procedia Cirp* 68, 358–362.

Prado-Cerqueira, J. L., Diéguez, J. L., and Camacho, A. M. (2017). Preliminary Development of a Wire and Arc Additive Manufacturing System (WAAM). *Procedia Manuf.* 13, 895–902. doi:10.1016/J.PROMFG.2017.09.154

Queguineur, A., Rückert, G., Cortial, F., and Hascoët, J. Y. (2018). Evaluation of Wire Arc Additive Manufacturing for Large-Sized Components in Naval Applications. *Weld. World* 62, 259–266. doi:10.1007/S40194-017-0536-8/FIGURES/16

Reisch, R., Hauser, T., Kamps, T., and Knoll, A. (2020). Robot Based Wire Arc Additive Manufacturing System with Context-Sensitive Multivariate Monitoring Framework. *Procedia Manuf.* 51, 732–739. doi:10.1016/J.PROMFG.2020.10.103

Rodrigues, T. A., Bairrão, N., Farias, F. W. C., Shamsolhodaei, A., Shen, J., Zhou, N., et al. (2022). Steel-copper Functionally Graded Material Produced by Twin-Wire and Arc Additive Manufacturing (T-WAAM). *Mater Des.* 213, 110270. doi:10.1016/J.MATDES.2021.110270

Rodrigues, T. A., Duarte, V. R., Miranda, R. M., Santos, T. G., and Oliveira, J. P. (2021). Ultracold-Wire and Arc Additive Manufacturing (UC-WAAM). *J. Mater Process Technol.* 296, 117196. doi:10.1016/J.JMATPROTEC.2021.117196

Sames, W. J., List, F. A., Pannala, S., Dehoff, R. R., and Babu, S. S. (2016). *The Metallurgy and Processing Science of Metal Additive Manufacturing*, 61, 315–360. doi:10.1080/09506608.2015.1116649

Sarma, R., Kapil, S., and Joshi, S. N. (2021). A Hybrid Slicing Method to Eliminate the Need of Support Structures in Direct Energy Deposition and Material Extrusion-Based Processes. *Springer Proc. Mater* 9, 299–312. doi:10.1007/978-981-16-0182-8_23/COVER/

Sarma, R., Kapil, S., and Joshi, S. N. (2022). Development of a Framework for Computer Aided Design and Manufacturing of 3 axis Hybrid Wire Arc Additive Manufacturing. *Mater Today Proc.* 62, 7625–7634. doi:10.1016/J.MATPR.2022.05.011

Sasikumar, R., Kannan, A. R., Kumar, S. M., Pramod, R., Kumar, N. P., Shanmugam, N. S., et al. (2022). Wire Arc Additive Manufacturing of Functionally Graded Material with SS 316L and IN625: Microstructural and Mechanical Perspectives. *CIRP J. Manuf. Sci. Technol.* 38, 230–242. doi:10.1016/J.CIRPJ.2022.05.005

Senthil, T. S., Ramesh Babu, S., Puviyarasan, M., and Dhinakaran, V. (2021). Mechanical and Microstructural Characterization of Functionally Graded Inconel 825 - SS316L Fabricated Using Wire Arc Additive Manufacturing. *J. Mater Res. Technol.* 15, 661–669. doi:10.1016/J.JMRT.2021.08.060

Shembekar, A. V., Yoon, Y. J., Kanyuck, A., and Gupta, S. K. (2019). Generating Robot Trajectories for Conformal Three-Dimensional Printing Using Nonplanar Layers. *J. Comput. Inf. Sci. Eng.* 19. doi:10.1115/1.4043013/726284

Shukla, P., Dash, B., Kiran, D. V., and Bukkapatnam, S. (2020). Arc Behavior in Wire Arc Additive Manufacturing Process. *Procedia Manuf.* 48, 725–729. doi:10.1016/J.PROMFG.2020.05.105

Song, X., Pan, Y., and Chen, Y. (2015). Development of a Low-Cost Parallel Kinematic Machine for Multidirectional Additive Manufacturing. *J. Manuf. Sci. Eng. Trans. ASME* 137. doi:10.1115/1.4028897/377512

Song, Y. A., Park, S., Choi, D., and Jee, H. (2005). 3D Welding and Milling: Part I–A Direct Approach for Freeform Fabrication of Metallic Prototypes. *Int. J. Mach. Tools Manuf.* 45, 1057–1062. doi:10.1016/J.IJMACHTOOLS.2004.11.021

Srivastava, S., Garg, R. K., Sharma, V. S., and Sachdeva, A. (20202020). Measurement and Mitigation of Residual Stress in Wire-Arc Additive Manufacturing: A Review of Macro-Scale Continuum Modelling Approach. *Arch. Comput. Methods Eng.* 28, 3491–3515. doi:10.1007/S11831-020-09511-4

Suárez, A., Aldalur, E., Veiga, F., Artaza, T., Tabernero, I., and Lamikiz, A. (2021). Wire Arc Additive Manufacturing of an Aeronautic Fitting with Different Metal Alloys: From the Design to the Part. *J. Manuf. Process* 64, 188–197. doi:10.1016/J.JMAPRO.2021.01.012

Sun, J., Yu, H., Zeng, D., and Shen, P. (2022). Wire–powder–arc Additive Manufacturing: A Viable Strategy to Fabricate Carbide Ceramic/aluminum Alloy Multi-Material Structures. *Addit. Manuf.* 51, 102637. doi:10.1016/J.ADDMA.2022.102637

Sun, R., Li, L., Zhu, Y., Guo, W., Peng, P., Cong, B., et al. (2018). Microstructure, Residual Stress and Tensile Properties Control of Wire-Arc Additive Manufactured 2319 Aluminum Alloy with Laser Shock Peening. *J. Alloys Compd.* 747, 255–265. doi:10.1016/J.JALLCOM.2018.02.353

Surappa, M. K. (20032003). Aluminium Matrix Composites: Challenges and Opportunities. *Sadhana* 28, 319–334. doi:10.1007/BF02717141

Suryakumar, S., Karunakaran, K. P., Chandrasekhar, U., and Somashekara, M. A. (2013). *A Study of the Mechanical Properties of Objects Built through Weld-Deposition*, 227, 1138–1147. doi:10.1177/0954405413482122

Szost, B. A., Terzi, S., Martina, F., Boisselier, D., Prytuliak, A., Pirling, T., et al. (2016). A Comparative Study of Additive Manufacturing Techniques: Residual Stress and Microstructural Analysis of CLAD and WAAM Printed Ti–6Al–4V Components. *Mater Des.* 89, 559–567. doi:10.1016/J.MATDES.2015.09.115

Tadge, P., Gupta, P. K., and Sasikumar, C. (2015). Surface Nano-Crystallizationof AISI 304 Stainless Steel through Shot Peening Technique. *Mater Today Proc.* 2, 3245–3250. doi:10.1016/J.MATPR.2015.07.133

Tian, Y., Shen, J., Hu, S., Han, J., Wang, Q., and Cai, Y. (2021). Effects of Ultrasonic Peening Treatment Layer by Layer on Microstructure of Components Fabricated by Wire and Arc Additive Manufacturing. *Mater Lett.* 284, 128917. doi:10.1016/J.MATLET.2020.128917

Veiga, F., Del Val, A. G., Suárez, A., and Alonso, U. (2020). Analysis of the Machining Process of Titanium Ti6Al-4V Parts Manufactured by Wire Arc Additive Manufacturing (WAAM). *Mater. (Basel)* 13. doi:10.3390/MA13030766

Wang, C., Suder, W., Ding, J., and Williams, S. (2021). The Effect of Wire Size on High Deposition Rate Wire and Plasma Arc Additive Manufacture of Ti-6Al-4V. *J. Mater Process Technol.* 288, 116842. doi:10.1016/J.JMATPROTEC.2020.116842

Wang, C., Suder, W., Ding, J., and Williams, S. (2021). Wire Based Plasma Arc and Laser Hybrid Additive Manufacture of Ti-6Al-4V. *J. Mater Process Technol.* 293, 117080. doi:10.1016/J.JMATPROTEC.2021.117080

Wang, J., Pan, Z., Ma, Y., Lu, Y., Shen, C., Cuiuri, D., et al. (2018). Characterization of Wire Arc Additively Manufactured Titanium Aluminide Functionally Graded Material: Microstructure, Mechanical Properties and Oxidation Behaviour. *Mater Sci. Eng. A* 734, 110–119. doi:10.1016/J.MSEA.2018.07.097

Wang, L., and Xue, J. (2017). Perspective on Double Pulsed Gas Metal Arc Welding. *Appl. Sci.* 7, 894. doi:10.3390/APP7090894

Wang, L. L., Wei, H. L., Xue, J. X., and DebRoy, T. (2018). Special Features of Double Pulsed Gas Metal Arc Welding. *J. Mater Process Technol.* 251, 369–375. doi:10.1016/J.JMATPROTEC.2017.08.039

Wang, X., Fan, D., Huang, J., and Huang, Y. (2014). A Unified Model of Coupled Arc Plasma and Weld Pool for Double Electrodes TIG Welding. *J. Phys. D. Appl. Phys.* 47, 275202. doi:10.1088/0022-3727/47/27/275202

Wang, Y., Zhang, Y., Song, G., Niu, W., Xu, Z., and Huang, C. (2020). Effect of Shot Peening on Fatigue Crack Propagation of Ti6Al4V. *Mater Today Commun.* 25, 101430. doi:10.1016/J.MTCOMM.2020.101430

Warsi, R., Kazmi, K. H., and Chandra, M. (2022). Mechanical Properties of Wire and Arc Additive Manufactured Component Deposited by a CNC Controlled GMAW. *Mater Today Proc.* 56, 2818–2825. doi:10.1016/J.MATPR.2021.10.114

Watanabe, T., Shiroki, M., Yanagisawa, A., and Sasaki, T. (2010). Improvement of Mechanical Properties of Ferritic Stainless Steel Weld Metal by Ultrasonic Vibration. *J. Mater Process Technol.* 210, 1646–1651. doi:10.1016/J.JMATPROTEC.2010.05.015

Weiss, L. E., Prinz, F. B., and Siewiorek, D. (1991). *A framework for thermal spray shape deposition: The MD* system. In "1991 International Solid Freeform Fabrication Symposium"*. The University of Texas in Austin.

Wen, T., Liu, S. Y., Chen, S., Liu, L. T., and Yang, C. (2015). Influence of High Frequency Vibration on Microstructure and Mechanical Properties of TIG Welding Joints of AZ31 Magnesium Alloy. *Trans. Nonferrous Met. Soc. China* 25, 397–404. doi:10.1016/S1003-6326(15)63616-0

Williams, S. W., Martina, F., Addison, A. C., Ding, J., Pardal, G., and Colegrove, P. (2016). *Wire + Arc Additive Manufacturing*, 32, 641. doi:10.1179/1743284715Y.0000000073

Wu, B., Ding, D., Pan, Z., Cuiuri, D., Li, H., Han, J., et al. (2017). Effects of Heat Accumulation on the Arc Characteristics and Metal Transfer Behavior in Wire Arc Additive Manufacturing of Ti6Al4V. *J. Mater Process Technol.* 250, 304–312. doi:10.1016/J.JMATPROTEC.2017.07.037

Wu, D., Guo, M., Ma, G., and Niu, F. (2015). Dilution Characteristics of Ultrasonic Assisted Laser Clad Yttria-Stabilized Zirconia Coating. *Mater Lett.* 141, 207–209. doi:10.1016/J.MATLET.2014.11.058

Wu, Q., Mukherjee, T., De, A., and DebRoy, T. (2020). Residual Stresses in Wire-Arc Additive Manufacturing – Hierarchy of Influential Variables. *Addit. Manuf.* 35, 101355. doi:10.1016/J.ADDMA.2020.101355

Wu, Y., and Kovacevic, R. (2005). *Mechanically Assisted Droplet Transfer Process in Gas Metal Arc Welding*, 216, 555–564. doi:10.1243/0954405021520247

Xiong, J., Lei, Y., Chen, H., and Zhang, G. (2017). Fabrication of Inclined Thin-Walled Parts in Multi-Layer Single-Pass GMAW-Based Additive Manufacturing with Flat Position Deposition. *J. Mater Process Technol.* 240, 397–403. doi:10.1016/J.JMATPROTEC.2016.10.019

Xiong, J., Lei, Y., and Li, R. (2017). Finite Element Analysis and Experimental Validation of Thermal Behavior for Thin-Walled Parts in GMAW-Based Additive Manufacturing with Various Substrate Preheating Temperatures. *Appl. Therm. Eng.* 126, 43–52. doi:10.1016/J.APPLTHERMALENG.2017.07.168

Xiong, J., Liu, G., and Pi, Y. (2019). Increasing Stability in Robotic GTA-Based Additive Manufacturing through Optical Measurement and Feedback Control. *Robot. Comput. Integr. Manuf.* 59, 385–393. doi:10.1016/J.RCIM.2019.05.012

Yang, Y., Jin, X., Liu, C., Xiao, M., Lu, J., Fan, H., et al. (2018). Residual Stress, Mechanical Properties, and Grain Morphology of Ti-6Al-4V Alloy Produced by Ultrasonic Impact Treatment Assisted Wire and Arc Additive Manufacturing. *Met* 8, 934. doi:10.3390/MET8110934

Yu, X., Lim, Y. C., Smith, R., Babu, S. S., Farson, D. F., Lippold, J. C., et al. (2014). *Reducing Hot Cracking Tendency of Dissimilar Weld Overlay by Magnetic Arc Oscillation*, 30, 930. doi:10.1179/1743284713Y.00000003587

Yu, Z., Yuan, T., Xu, M., Zhang, H., Jiang, X., and Chen, S. (2021). Microstructure and Mechanical Properties of Al-Zn-Mg-Cu Alloy Fabricated by Wire + Arc Additive Manufacturing. *J. Manuf. Process* 62, 430–439. doi:10.1016/J.JMAPRO.2020.12.045

Yuan, T., Kou, S., and Luo, Z. (2016). Grain Refining by Ultrasonic Stirring of the Weld Pool. *Acta Mater* 106, 144–154. doi:10.1016/J.ACTAMAT.2016.01.016

Yuan, T., Luo, Z., and Kou, S. (2016). Grain Refining of Magnesium Welds by Arc Oscillation. *Acta Mater* 116, 166–176. doi:10.1016/J.ACTAMAT.2016.06.036

Zhang, Z., Sun, C., Xu, X., and Liu, L. (2018). Surface Quality and Forming Characteristics of Thin-Wall Aluminium Alloy Parts Manufactured by Laser Assisted MIG Arc Additive Manufacturing. *Int. J. Light Mater Manuf.* 1, 89–95. doi:10.1016/J.IJLMM.2018.03.005

Zhang, C., Li, Y., Gao, M., and Zeng, X. (2018). Wire Arc Additive Manufacturing of Al-6Mg Alloy Using Variable Polarity Cold Metal Transfer Arc as Power Source. *Mater Sci. Eng. A* 711, 415–423. doi:10.1016/J.MSEA.2017.11.084

Zhang, J., Jian, Y., Zhao, X., Meng, D., Pan, F., and Han, Q. (2021). The Tribological Behavior of a Surface-Nanocrystallized Magnesium Alloy AZ31 Sheet after Ultrasonic Shot Peening Treatment. *J. Magnes. Alloy* 9, 1187–1200. doi:10.1016/J.JMA.2020.11.012

Zhang, S., Gong, M., Zeng, X., and Gao, M. (2021). Residual Stress and Tensile Anisotropy of Hybrid Wire Arc Additive-Milling Subtractive Manufacturing. *J. Mater Process Technol.* 293, 117077. doi:10.1016/J.JMATPROTEC.2021.117077

Zhang, S., Zhang, Y., Gao, M., Wang, F., Li, Q., and Zeng, X. (2019). *Effects of Milling Thickness on Wire Deposition Accuracy of Hybrid Additive/subtractive Manufacturing*, 24, 375–381. doi:10.1080/13621718.2019.1595925

Zhang, T., Li, H., Gong, H., Ding, J., Wu, Y., Diao, C., et al. (2022). Hybrid Wire - Arc Additive Manufacture and Effect of Rolling Process on Microstructure and Tensile Properties of Inconel 718. *J. Mater Process Technol.* 299, 117361. doi:10.1016/J.JMATPROTEC.2021.117361

Zhang, W., Ding, C., Wang, H., Meng, W., Xu, Z., and Wang, J. (2021). The Forming Profile Model for Cold Metal Transfer and Plasma Wire-Arc Deposition of Nickel-Based Alloy. *J. Mater Eng. Perform.* 30, 4872–4881. doi:10.1007/S11665-021-05485-X/FIGURES/12

Zhang, X., Wang, K., Zhou, Q., Ding, J., Ganguly, S., Grasso, M., et al. (2019). Microstructure and Mechanical Properties of TOP-TIG-Wire and Arc Additive Manufactured Super Duplex Stainless Steel (ER2594). *Mater Sci. Eng. A* 762, 138097. doi:10.1016/J.MSEA.2019.138097

Zhang, Y. M., Li, P., Chen, Y., and Male, A. T. (2002). Automated System for Welding-Based Rapid Prototyping. *Mechatronics* 12, 37–53. doi:10.1016/S0957-4158(00)00064-7

Zhao, D., and Guo, W. (2020). Mixed-layer Adaptive Slicing for Robotic Additive Manufacturing (AM) Based on Decomposing and Regrouping. *J. Intell. Manuf.* 31, 985–1002. doi:10.1007/S10845-019-01490-Z/TABLES/2

Zhou, J., Jia, C., Guo, M., Chen, M., Gao, J., and Wu, C. (2021). Investigation of the WAAM processes features based on an indirect arc between two non-consumable electrodes *Vacuum* 183 (4), 109851. doi:10.1016/j.vacuum.2020.109851

Zhou, J., Xu, J., Huang, S., Hu, Z., Meng, X., and Fan, Y. (2017). *Microstructure and Mechanical Properties of Cr12MoV by Ultrasonic Vibration-Assisted Laser Surface Melting*, 33, 1200–1207. doi:10.1080/02670836.2016.1273989